Available online at www.sciencedirect.com

SciVerse ScienceDirect

journal homepage: www.elsevier.com/locate/he

Photo-induced reforming of alcohols with improved hydrogen apparent quantum yield on TiO_2 nanotubes loaded with ultra-small Pt nanoparticles

Mariana P. Languer [a], *Francine R. Scheffer* [a], *Adriano F. Feil* [b,c], *Daniel L. Baptista* [b], *Pedro Migowski* [a], *Guilherme J. Machado* [b], *Diogo P. de Moraes* [a], *Jairton Dupont* [a], *Sérgio R. Teixeira* [b], *Daniel E. Weibel* [a,*]

[a] *Instituto de Química, Universidade Federal do Rio Grande do Sul, UFRGS, Avenida Bento Gonçalves 9500, P.O. Box 15003, 91501-970 Porto Alegre, RS, Brazil*

[b] *Instituto de Física, Universidade Federal do Rio Grande do Sul, UFRGS, Avenida Bento Gonçalves 9500, P.O. Box 15051, 91501-970 Porto Alegre, RS, Brazil*

[c] *Faculdade de Física, Pontifícia Universidade Católica do Rio Grande do Sul (PUCRS), Avenida Ipiranga 6681, 90619-900 Porto Alegre, RS, Brazil*

ARTICLE INFO

Article history:
Received 1 July 2013
Received in revised form
1 September 2013
Accepted 4 September 2013
Available online 2 October 2013

Keywords:
Photocatalysis
Water splitting
Hydrogen production
TiO_2 nanotubes
Platinum
Apparent quantum yield

ABSTRACT

Photo-induced reforming of methanol, ethanol, glycerol and phenol at room temperature for hydrogen production was investigated with the use of ultra-small Pt nanoparticles (NPs) loaded on TiO_2 nanotubes (NTs). The Pt NPs with diameters between 1.1 and 1.3 nm were deposited on TiO_2 NTs by DC-magnetron sputtering (DC-MS) technique. The photocatalytic hydrogen rate achieved an optimum value for a loading of about 1 wt% of Pt. Apparent quantum yield for hydrogen generation was measured for methanol and ethanol water solutions reaching a maximum of 16% under irradiation with a wavelength of 313 nm in methanol/water solution (1/8 v/v). Pt NPs loaded on TiO_2 NTs represented also a true water splitting catalyst under UV irradiation and pure distilled water. DC-MS method appears to be a technologically simple, ecologically benign and potentially low-cost process for production of an efficient photocatalyst loaded with ultra-small NPs with precise size control.

1. Introduction

Photocatalytic hydrogen production via photocatalysis has great potential for solving environmental and energy issues and has been the focus of increasing research in the last decade. In particular, heterogeneous photocatalytic reactions on TiO_2 semiconductors have been attracting much attention because of their potential applications in hydrogen

* *Corresponding author*. Tel.: +55 5133086204; fax: +55 5133087304.
E-mail address: danielw@iq.ufrgs.br (D.E. Weibel).

0360-3199/$ – see front matter
http://dx.doi.org/10.1016/j.ijhydene.2013.09.018

production by water splitting (WS) and environmental clean-up by the so-called advanced oxidative processes (AOP) [1,2]. The WS reaction was discovered in 1972 [3], and after more than 40 years, no real breakthroughs have been observed in the field. The WS reaction, referred to as one of the "holy grail" [4] of chemistry, remains elusive in spite of the exponential growth of scientific articles that have been published in the last decade. In spite of promising results that have been reported, a commercially viable catalyst system for this transformation is still absent, even for the high surface area TiO_2 nanotubes (NTs). This difficulty is mainly due to the rapid recombination of photogenerated conduction-band electrons and valence band holes summed to the efficient surface recombination back-reaction of oxygen and hydrogen to produce water [5].

Photogeneration of hydrogen from water is usually investigated, contrary to AOPs, in unaerated conditions with simultaneous hydrogen production rate enhanced by the use of the so called sacrificial agents [5]. These agents increase the life time of the photoelectrons, decreasing the rate of electron–hole recombination and increasing consequently the hydrogen generation yield. In this sense, if the sacrificial agent is a pollutant present in the wastewater there is a possibility of the organic pollutant degradation together with hydrogen generation. In the last decade there have been used a large variety of electron donors for photocatalytic hydrogen production, such as alcohols [6–9], polyalcohols [10,11], sugars [12], n-heptane cracking [13] and chloroacetic acids [14]. Within all the above series of sacrificial agents, alcohols were found to be very efficient as hole scavengers increasing the hydrogen production rate one or two orders of magnitude compared to the WS reaction carried out in pure water. For this reason a number of research groups have recently moved their attention to the study of hydrogen production over TiO_2 nanoparticles together with pollutant degradation [8,10,14,15]. The results were promising, especially because the overall process can be described as a photo-induced reform of alcohols at room temperature representing an environmentally friendly and low cost method for wastewater treatment with simultaneous production of clean and renewable energy source, i.e., hydrogen.

Photocatalytic activity can be increased, for example, by the presence of Pt nanoparticles (NPs) [7,10,16–18] or Gold NPs [19–22] as co-catalyst deposited on TiO_2 surface. Several works have reported new Pt-loaded photocatalysts with improve efficiency towards water splitting using TiO_2 NTs structures [23,24]. The photocatalytic reaction over Pt/TiO_2 systems has been already studied from the point of view of pollutant degradation [8] and also for the production of hydrogen [7,8,10,25–28]. After the absorption of the photon and charge separation, the photocatalytic reaction requires that the photogenerated electrons in the conduction band of TiO_2 migrate to the Pt NPs through the Pt/TiO_2 interfaces. The electrons finally are trapped by the Pt particles and available to participate in reduction reactions. The holes generated in the valence band remain for oxidation reactions [7]. The low-charge separation and transfer efficiency constitutes the bottle neck of the process where an intense electron–hole recombination takes place. If a sacrificial agent is present in the water and the electron transfer at the Pt/TiO_2 interface is efficient, high production rates should be expected. The photocatalytic hydrogen production from aqueous methanol solutions over Pt-loaded laboratory prepared TiO_2, non nonstoichiometric titania oxide and commercial TiO_2 photocatalysts has been recently studied [26,29]. In particular, Kandiel et al. [26] obtained interesting results using methanol as hole scavenger, indicating that this system should be described as a methanol dehydrogenation reaction when the photocatalytic reaction is stopped at the first step of photocatalytic oxidation (formaldehyde formation). Then when carbon dioxide is detected the photocatalytic reaction would be described better as methanol reforming but not as a real water splitting system.

The amount of Pt can play a key role in deciding whether a particular catalyst has a positive, negative or even null photocatalytic effect. Several authors have observed that an optimal loading of Pt existed for promoting photocatalytic rates on TiO_2 surfaces and Pt loading over about 1 wt% resulted in attenuation of photochemical rates as a result of blocking of the TiO_2 surface [8,10,16,30,31]. Several ways of Pt deposition have been used over the years; among them photoassisted Pt deposition [16,32,33] and in particular the wet impregnation method were employed due to its simplicity [7,16,25,34]. Wet impregnation methodology, the more common approach used, has a poor control on the amount and type of Pt nanoparticles deposited on the TiO_2 structures. For this reason, a number of groups starting to use sputtering deposition methods to control the amount of Pt loading with precision [30,31,35]. In spite Platinum has a high price and limited world-wide supply, recently it was shown that the sputtering method allow to use a minimum metal loading without compromise efficiency [36].

Herein we extend our previous work on hydrogen production by NTs photocatalysts [37–39] loading ultra-small Pt NPs on TiO_2 NTs by DC-magnetron sputtering deposition (DC-MS) method. Photocatalytic hydrogen generation under UV irradiation using methanol, ethanol, glycerol and phenol as sacrificial species was investigated. Hydrogen apparent quantum efficiencies (Φ_{app}), using methanol and ethanol as typical hole scavengers to enhance hydrogen production rate, were also measured. The prepared photocatalysts showed Φ_{app} of 16% at an excitation wavelength of 313 nm for thin 1.5 μm length TiO_2 NTs. The Pt NPs loaded on TiO_2 NTs reported here represents also a true WS catalyst under UV irradiation and pure distilled water.

2. Experimental section

2.1. *Preparation and characterization of TiO_2 photocatalysts*

TiO_2 NTs were prepared by anodization of a Ti foil with constant applied voltage at room temperature, using an electrolyte containing ethylene glycol + 0.25 wt% NH_4F + 10 wt% H_2O with ultrasonic bath following a methodology already described [37–40]. After the anodization the TiO_2 NTs were annealed at 400 °C for 3 h in air atmosphere in order to crystallize the oxide nanotubes layer. The crystal structure analyses of TiO_2 NTs after thermal treatment was performed by Rietveld profile refinement using Fullprof software [41]. For

the Rietveld refinements, a preferred orientation (Ph) using the Modified March's function was used [42,43] (eq. (1)):

$$P_h = G_2 + (1 - G_2)\left((G_1 \cos\alpha_h)^2 + \frac{\sin^2\alpha_h}{G_1}\right)^{-3/2} \quad (1)$$

where G_1 correspond to the Bragg–Brentano geometry, G_2 represents the fraction of the sample without orientation and α_h is the acute angle between the scattering vector and the normal to the crystallites.

Pt NPs loaded on TiO_2 NTs were prepared by DC-magnetron sputtering (DC-MS) deposition method. The deposition was performed in a sputter coater MED 020 (Bal-Tech). Initially the vacuum chamber was evacuated at 10^{-4} Pa. The Pt deposition was carried out under an argon work pressure of 2.0 Pa at room temperature, with discharge current of 40 mA for 6 s. The TiO_2 NTs surface was located at a distance of 50 mm from the Pt target (99.99% in purity). The control of deposition rate was performed in situ by a quartz crystal film thickness measurement device (QSG 060 - Bal-Tech). Platinum determination was carried out following a standard procedure using a flame atomic absorption spectrometer (Analyst 200, PerkinElmer, Singapore) equipped with a deuterium background corrector and a hollow cathode lamp of Pt (wavelength of 265.95 nm and current of 30 mA). High resolution transmission electron microscopy (HRTEM) analyses were carried out in a Cs-corrected FEI Titan 80/300 transmission electron microscope, equipped with an energy dispersive X-ray (EDX) analyzer at INMETRO, Brazil. High Z-contrast images were acquired through scanning transmission electron microscopy (STEM) using a high-angle annular dark-field detector. The mean size of Pt NPs was obtained averaging the measurements of 300 NPs. For each Pt NPs the two longest diameters were measured, therefore 600 measurements were averaged to obtain the final mean diameter informed. The EDX analyses were performed in STEM mode, allowing nanometer scale spatial resolution. Glancing angle X-ray diffraction (GAXRD) patterns were recorded at the Laboratório Nacional de Luz Síncrotron (LNLS, XRD-2 beam line, $\lambda = 1.50$ Å, Campinas, Brazil). The sample was tilted in an angle ω fixed in 2° and the GAXRD measurements was realized in a 2θ range from 10 to 80° with a 0.02° step size and measuring time of 20 s per step.

High resolution X-ray photoelectron spectroscopy (XPS) Pt 4f spectra were obtained with 10 eV of pass energy at the TGM (Toroidal Grating Monochromator) beam line of the LNLS, Campinas, Brazil. XPS spectra were obtained using a high performance hemispheric SPECSLAB II (Phoibos-Hs 3500,150 analyzer, SPECS) energy analyzer. Alternatively, XPS spectra were also obtained using a conventional electron spectrometer (Omicron N. T.Gmbh, Germany) and a non-monochromatic Al Kα radiation as excitation source. Pass energies of 50 eV and 10 eV were used for the survey, and single element spectra, respectively. The position of the C 1s signal corresponding to C–C/C–H was always used for energy calibration, by setting the energy value at 285.0 eV. The envelopes were analyzed and peak-fitted after subtraction of the Shirley background using Gaussian–Lorenzian peak shapes obtained from the CasaXPS software package.

2.2. Photocatalytic hydrogen measurements

Hydrogen photogeneration experiments were carried out in a calibrated (22.16 ± 0.01) mL gas-closed photochemical reactor made of PTFE under continuous magnetic stirring (see Figure S1, in supporting information). A quartz window of 2.54 cm in diameter allowed irradiation of the aqueous mixture under a wide incident spectral range, including UV and visible light. The photocatalysis was carried out with unfiltered or filtered light from a high pressure Xe/Hg lamp 150 W (Sciencetech Inc.). Wavelengths were selected using line filters of ±10 nm FWHM (Newport). A precision Iris was set in the output of the line filter box to allow only irradiation on the NTs surface. Prior to irradiation, the reactor was deaerated with nitrogen or argon. The photocatalytic activity of the titania NTs were evaluated by gas chromatography (Agilent 6820 GC chromatograph) using a molecular sieve 5Å packed column following the procedure previously reported [39]. As the mixture of methanol and water has a partial molar volume which depends on the concentration of methanol and water, the actual volume of the mixture was determined by measuring the density of the final mixture and the remaining gas volume was corrected accordingly. This correction was only carried out for water/methanol mixtures where Φ_{app} was measured. Actinometry measurements were performed initially, and at the end of a photochemical run. When it was necessary, the intensity of the light was controlled at intermediate times during the photocatalysis. An average value of the light intensities was used for quantum yield calculations. The relative intensities at the wavelength selected 254, 313 and 365 nm were approximately 1, 3 and 9 respectively. The quantum yield of the actinometer, potassium ferrioxalate, was assumed to be 1.25 at all wavelengths studied [44]. It was considered also that 100% of the photons reaching the surface of the NTs were absorbed. Due to the TiO_2 NTs array studied here have 1.5 μm thicknesses, the 100% absorption approximation is valid [27]. Since production of hydrogen is a two electron process,

$$2H^+ + 2e^- \rightarrow H_2 \quad (2)$$

Φ_{app} is defined as twice the number of hydrogen molecules produced divided by the number of absorbed incident photons. The photocatalytic data presented here for Pt loaded on TiO_2 NTs corresponded to 6 s of deposition time, which produced a hydrogen rate close to the maximum obtained under the present experimental conditions. Because the maximum photoactivity for Pt loaded TiO_2 (usually in the form of P-25) is obtained with about 1% w/w% of Pt, the measurements of Φ_{app} were carried out using NTs loaded with 0.7% w/w% of Pt (6 s of sputtering).

3. Results and discussion

3.1. Photocatalyst characterization

The TiO_2 NTs substrates after annealed at 400 °C for 3 h in air atmosphere showed a typical crystalline anatase phase. Fig. 1 shows the GAXRD patterns of the as-anodized TiO_2 NTs and annealed TiO_2 NTs, respectively. The results show that as-anodized sample present an amorphous TiO_2 structure

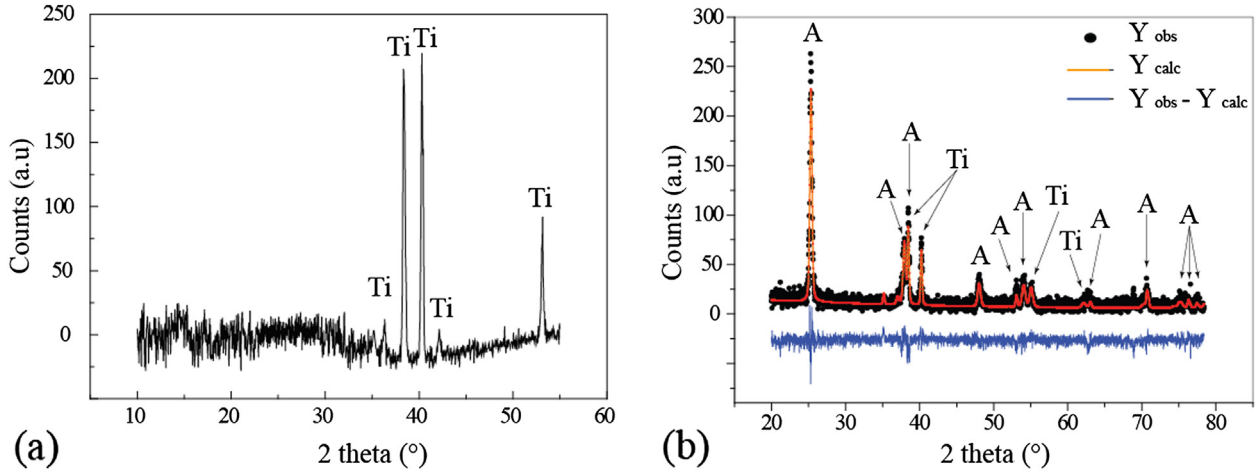

Fig. 1 – XRD diffractograms of the (a) as-anodized and (b) annealed TiO_2 NTs. The NTs were annealed at 400 °C for 3 h in air atmosphere. A = anatase and Ti = titanium.

(Fig. 1a) and after the annealing process only tetragonal anatase structure was formed (Fig. 1b). The Rietveld refinement indicated that the average size of the anatase crystallites structure presented 31.64 nm and lattice parameters of $a = 3.789$, $b = 3.789$ and $c = 9.490$ Å.

Field Emission Scanning Electron Microscopy (FESEM) microscopy images of the TiO_2 NTs with 1.5 μm length, 70 nm diameter and ~10 nm wall thickness can be seen in Fig. 2a–b. After annealing, TiO_2 NTs samples were loaded with ultra-small Pt NPs by DC-MS for 2, 6 and 12 s. The Pt quantities deposited on the NTs were proportional to the deposition time. For example, the Pt amounts determined by atomic absorption spectroscopy were 0.7 and 1.6 w/w% for 6 s and 12 s of deposition time respectively. Fig. 2c shows representative STEM with high-Z contrast of the TiO_2 NTs decorated with Pt by sputtering for 12 s. HRTEM micrographs of the same sample can be seen in Fig. 2d. The inverse Fourier transform picture (Fig. 2e) obtained by treating the HRTEM image of a single Pt particle, shows the distance of 2.26 Å typical from the Pt (111) planes. EDX spectrum, Fig. 2f, confirms the presence of Pt in the sample as well as Ti and O from TiO_2 and Cu from the copper grid used on TEM analysis. Pt NPs sizes slightly increased from 1.1 ± 0.3 to 1.3 ± 0.3 nm when the sputtering time changed from 2 to 12 s (see Fig. 3).

Finally, XPS spectroscopy was used to prove the surface chemistry changes before and after Pt deposition. Following anodization, XPS survey spectra showed the presence of C, O, Ti, N and a small amount of F with an O/Ti ratio of 2.5–2.8 due to the presence of the electrolyte compounds on the surface. After the annealing process, F and N signal disappeared; leaving only carbon adventitious and an O/Ti ratio of about 2 (see Fig. S2 in supporting information). When Pt was deposited for 6 s a typical XPS spectrum of the Pt 4f region was measured (Fig. 4-top). Pt 4f electron spectrum is well-resolved with two main

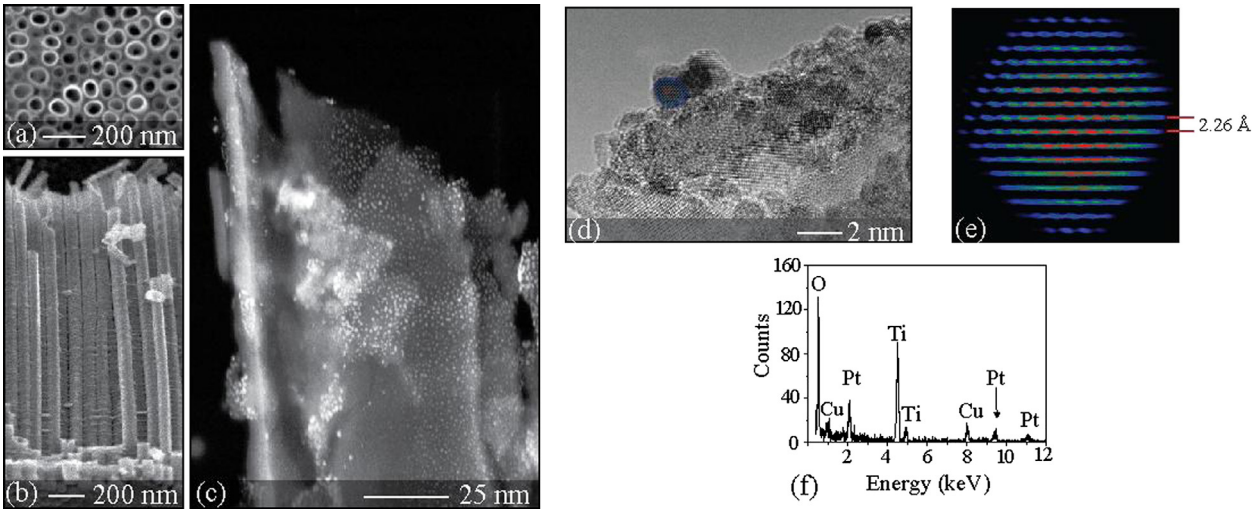

Fig. 2 – (a–b) FESEM of the TiO_2 NTs after annealing at 400 °C for 3 h in air atmosphere. (c–d) STEM microscopy of the High Z-contrast and HRTEM images of the ultra-small Pt NPs loaded on TiO_2 NTs, respectively. (e) Inverse Fourier transform image of the Pt (111) plane showing the distance of the crystalline planes (2.26 A). (f) EDX spectrum of the chemical composition of the ultra-small Pt NPs loaded on TiO_2 NTs system.

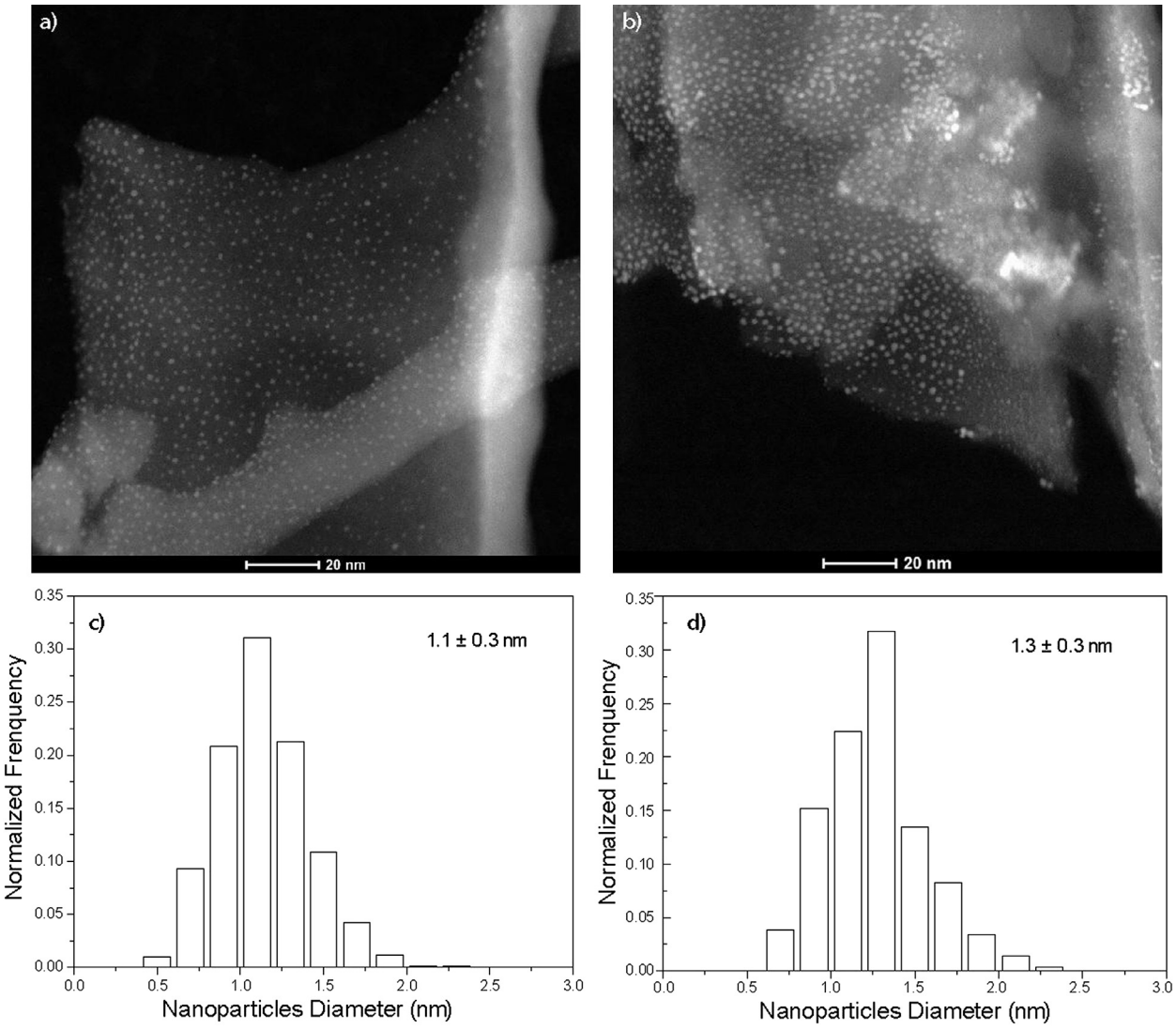

Fig. 3 – STEM images of the TiO_2 NTs decorated with (a) 2 s and (b) 12 s of Pt sputtering and corresponding size distribution histogram of the Pt nanoparticles ((c) 2 s and (d) 12 s of sputtering respectively).

doublets with Pt $4f_{7/2}$ and $4f_{5/2}$ binding energies between 71.2 and 74.5 eV. Both components of equal half-widths have an intensity ratio of ca. 4:3 and a separation of about 3.3 eV, very close to that it would be expected theoretically. These mains doublet signals (relative area ~86%) are undoubtedly due to Pt(0). Additional contributions at 72.7 and 75.8 eV are necessary to fit the experimental Pt 4f peak correctly that are assigned to PtO $4f_{7/2}$ and $4f_{5/2}$ respectively [34,45]. After photocatalysis the Pt 4f signal shows that about 28% of the Pt NPs deposited on TiO_2 NTs are oxidized and new signals at 74.1 and 77.2 eV appear in the XPS spectra that are assigned to PtO_2 $4f_{7/2}$ and $4f_{5/2}$ respectively (see Fig. 4-bottom). The higher binding energy component due to Pt(IV) species can be assigned to PtO_2 or $Pt(OH)_4$ [45].

3.2. *Alcohols photo-reforming and hydrogen production*

3.2.1. *Methanol and ethanol*

Methanol and ethanol are efficient hole scavengers and they are potential hydrogen "reservoirs" at ~12.5 and 13.0 wt% respectively. In spite they are frequently used as electron donor in so-called "sacrificial systems" for the photocatalytic H_2 production; only a few mechanistic study of this system have been published [46]. There is a very recent report concerning the quantum efficiency on the rate of the photocatalytic H_2 evolution over Pt-loaded TiO_2 NPs from aqueous methanol solution [26]. With respect to similar studies on pure TiO_2 NTs the information is lacking. Table 1 shows the enhancement of the H_2 production rate with the increase in methanol concentration. As the methanol concentration increased there was a proportional increase in hydrogen evolution rate. The hydrogen produced under UV irradiation on TiO_2 NTs was previously observed to evolve steadily and without decrease in the rate over long periods of time [39].

Typical results obtained in the presence of ethanol-water solutions on TiO_2 NTs are shown in Fig. 5 where the hydrogen production rate is plotted as functions of the irradiation time. The amount of evolved H_2 ($\mu mol\ cm^{-2}\ h^{-1}$) calculated from da data presented in Fig. 5 can be seen in

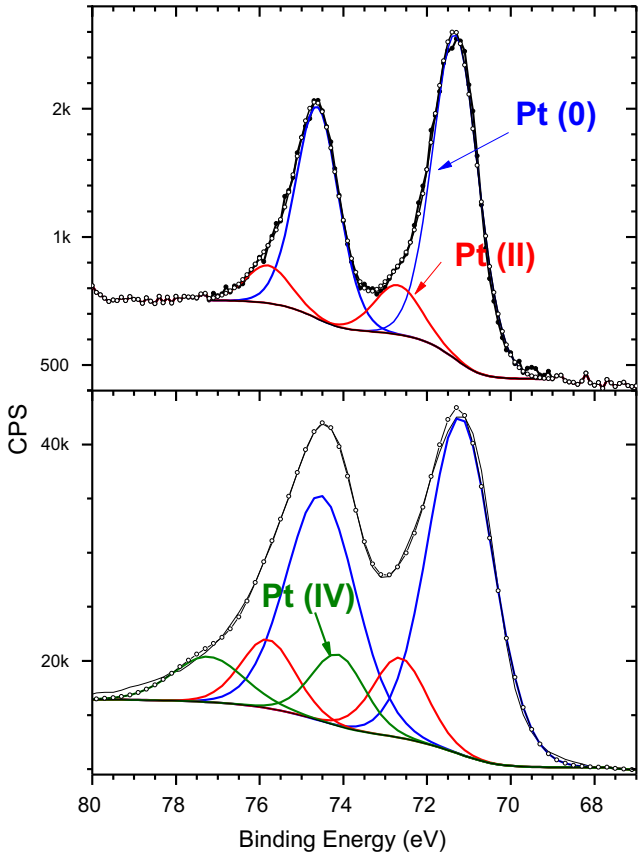

Fig. 4 – Typical Pt 4f XPS spectra of TiO_2 NTs samples loaded with the ultra-small Pt NPs before (top) and after photocatalysis (bottom).

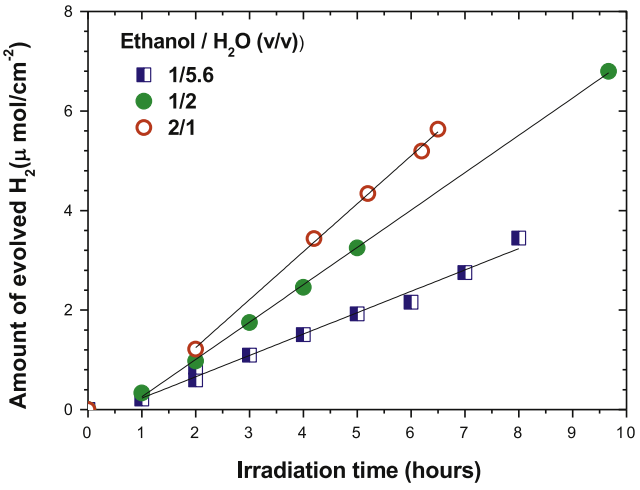

Fig. 5 – Amount of the photocatalytic hydrogen generation as a function of UV irradiation time on TiO_2 NTs photocatalyst for ethanol/water (v/v) solutions.

Table 1. The hydrogen rate also increased when the ethanol concentration increased. It can be observed in Table 1 that in the presence of ethanol the rate of hydrogen evolution is slightly lower than methanol, at similar concentrations. This small decrease in the hydrogen generation rate was already found when TiO_2 nanoparticles (P-25) were used (results not shown). This effect in the alcohol molecular size can be correlated with the electron transfer rate from trapped holes in TiO_2 that depend on the alcohol type. Tamaki et al. observed electron transfer times of ~100 ps for methanol, ~1 ns for ethanol and ~3 ns for isopropanol [47].

Table 1 – Photocatalytic hydrogen evolution over pure TiO_2 NTs arrays in the presence of several methanol and ethanol concentrations.

Mixture	Alcohol/H_2O (v/v)	Rate of evolved H_2 (μmol cm^{-2} h^{-1})
Only water	–	≤0.005
Methanol	1/17	0.13
	1/8	0.28
	1/3.5	0.46
Ethanol[a]	1/5.6	0.43
	1/2	0.75
	2/1	0.98

[a] Data obtained from Fig. 5.

3.2.2. *Glycerol and phenol*

Glycerol and Phenol have particular interests in reform them to hydrogen at room temperature using photocatalysis. In Brazil the diesel by Federal law contain 3% of biodiesel and in 2013 it has to contain 5% [48]. Brazil will produce 250,000 tons of glycerol per year. The annual consume of glycerol in Brazil is 30,000 tons and the large surplus will produce a pressure on the search for new commercial uses of glycerol. Similar tendency can be expected in others countries and reforming of glycerol by photocatalysis begun to be studied recently by using TiO_2 NPs [10,49]. Phenol and its derivates have been studied during decades using mainly commercially available TiO_2 NPs although recently new catalyst have been introduced [50–53]. In spite there is a wide range of research on phenol photodegradation processes, a hydrogen generation study on the diverse catalyst used during photodegradation is lacking. Therefore, it is of interest to know if there is any hydrogen production when phenol, a prototype well studied contaminant, is decomposed by photocatalysis.

Typical results on hydrogen photocatalytic generation in the presence of glycerol or phenol using TiO_2 NTs are shown in Fig. 6. The top of Fig. 6 shows that in the presence of glycerol the hydrogen rate formation is about 0.2 μmol h^{-1} cm^{-2}. This rate of hydrogen generation is lower than ethanol at a similar concentration and this should be expected when a larger alcohol molecule is used as sacrificial compound. Prolonged exposure to illumination results in the formation of CO and CO_2 as minor products of the photocatalytic reaction (the complete study on Glycerol photodegradation is going to be published elsewhere). The presence of CO_2 as final product of the mineralization reaction of Glycerol was already measured on TiO_2 and Pt/TiO_2 nanoparticles [10].

Fig. 6-bottom shows that a solution of 50 mg/L of phenol in water produce hydrogen at a rate of about 0.06 μmol h^{-1} cm^{-2},

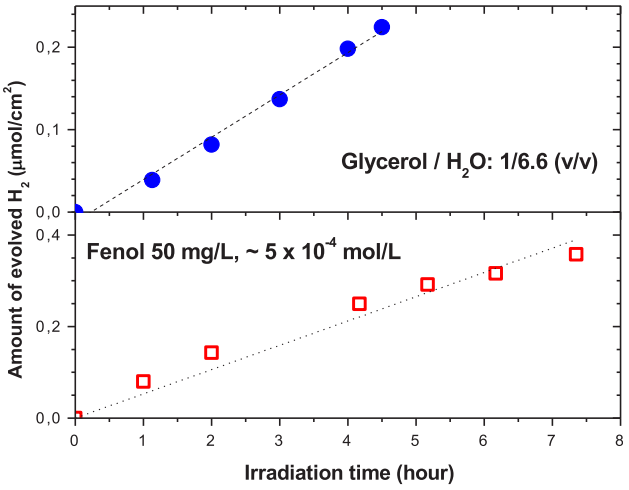

Fig. 6 – Evolution of photocatalytic hydrogen as a function of UV irradiation time for Glycerol/water (top) and phenol/water (bottom) solutions using TiO_2 NTs.

that is about 12 times higher than pure water. The data presented in Fig. 6-bottom is pointing out a fact that in a standard photodegradation process of phenol, and may be in the phenol family of compounds, hydrogen generation proceeds together with the photodegradation process in anaerobic conditions.

3.3. *Effect of Pt loading on the photocatalytic activity of TiO_2 NTs*

Results obtained from pure water and methanol/water solutions (1/8 v/v) on Pt-loaded TiO_2 and pure TiO_2 NTs are shown in Fig. 7. It is possible to observe that the rate of hydrogen

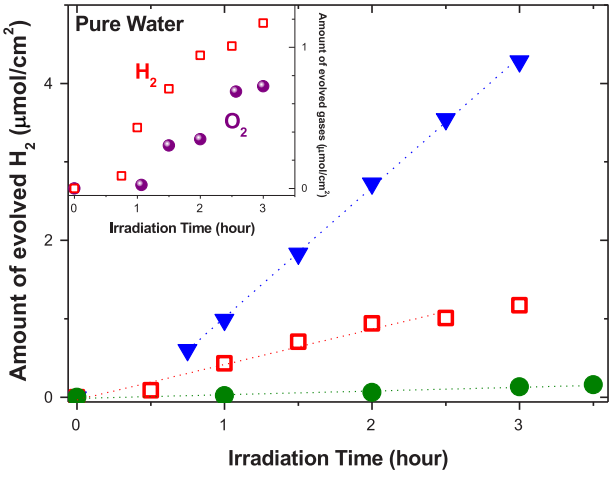

Fig. 7 – Photogeneration of hydrogen obtained from methanol/water solutions (1/8 v/v) and pure water for TiO_2 and Pt-loaded TiO_2 NTs. Close triangles: Pt-loaded TiO_2 NTs in methanol/water solution; open squares Pt-loaded TiO_2 NTs in pure distilled water and close circles: pure TiO_2 NTs in methanol/water solution. Inset: photogeneration of hydrogen and oxygen obtained from pure distilled water on Pt-loaded TiO_2 NTs.

production strongly increased when Pt was deposited on the TiO_2 NTs and that increase is even higher when methanol is present in the water. Taken into account the relative hydrogen evolution rates (Fig. 7) for pure TiO_2 NTs in methanol/water solution (close circles), Pt-loaded TiO_2 NTs in pure distilled water (open squares) and Pt-loaded TiO_2 NTs in methanol/water solution (close triangles); the relative rates are 1, 10 and 36 respectively. The rate of hydrogen generation in pure water using Pt-loaded TiO_2 NTs is much higher than TiO_2 NTs without Pt (compare data on Table 1 with Fig. 7). Nonetheless, Pt-loaded TiO_2 NTs in pure water have a ten times higher rate than pure TiO_2 NTs in contact with a methanol/water solution. The ultra-small Pt NPs loaded on TiO_2 NTs under UV radiation constitutes a real water splitting system producing hydrogen and oxygen gases under illumination (see inset of Fig. 7). The obtained results show that Pt NPs deposited on the TiO_2 NTs arrays resulted in a highly efficient system to produce hydrogen even in pure water. Recently, enhanced water photocatalysis with Pt metal nanoparticles on single crystal TiO_2 surfaces were obtained using a similar sputtering method [54]. Homogenous distributions of Pt NPs deposited onto columnar TiO_2 films from 1.15 to 3.46 nm were observed by HRTEM. This very recent report and the work presented here are pointing out the importance of size and surface distribution of small Pt NPs on hydrogen photogeneration reactions.

3.4. *Apparent quantum yield determination*

The intense research work developed in less than a decade on the water splitting reaction and the need to publish quickly new experimental results in this expanding field resulted in a serious problem: hydrogen production rates obtained with different catalyst, different excitation sources with a wide range of intensities and wavelengths, different active surface area (in general not known), several reactor geometries, etc. lead to quantitative comparisons between catalysts almost impossible. In the photochemical field a basic experimental determination to obtained information about mechanisms and kinetic processes is quantum yield measurements of products [55,56]. The knowledge of this parameter is fundamental. It enables one (i) to compare the activity of different catalysts for the same reaction, (ii) to estimate the relative feasibility of different reactions, and (iii) to calculate the energetic yield of the process and the corresponding cost. In heterogeneous photocatalysis, mainly due to scattering of the radiation, the apparent quantum yield (lower than the actual quantum yield) is a very useful quantitative measurement that it was almost forgotten in the last 15 years. Serpone, N. in a special communication to the editor in 1997 [57], invited to the readers to determine quantum yields in heterogeneous photocatalysts with the same or other equivalent approach to debate and understand the photocatalytic reactions on the same quantitative bases. However, the actual scientific communication of the experimental results and new discoveries in the field lack of Serpone thinking, and in consequence, it is very difficult to compare the enormous number of new catalytic systems that are synthesized every year.

The apparent quantum yield of hydrogen evolution on TiO_2 NTs and Pt/TiO_2 NTs was measured in a solution of methanol/

water (1/8 v/v). Particular care was taken to keep all the experimental optical parameters constant for the series of measurements. Φ_{app} have been determined at 254, 313 and 365 nm and the results are shown in Table 2. Examination of Φ_{app} of Table 2 shows that irradiation of pure TiO_2 NTs present a low Φ_{app} ranging from about 0.02% to 0.1% depending on the excitation wavelength. In this regard photocatalytic water splitting, even with sacrificial species, is a challenging process due to the low efficiency of the many systems that have been reported [2,58]. The results on pure TiO_2 NTs also showed an interesting property of the photochemical reaction on the NTs arrays: an apparent dependence with the excitation wavelength. When the wavelength decreased, Φ_{app} seemed to increase slightly.

When Pt was loaded on TiO_2 NTs arrays, Φ_{app} increased from 50 up to 800 times compared to pure TiO_2 NTs depending on the excitation wavelength (see Table 2). The high apparent quantum yields obtained are probably due to a synergy between the small size and homogenous surface distribution of the Pt NPs (see Figs. 2c and 3) produced by sputtering and the nanotubular geometry of the TiO_2 semiconductor. When ethanol was used as sacrificial specie a high Φ_{app} was also observed. In spite, the Φ_{app} of hydrogen production without Pt NPs in ethanol solutions were not measured, a very low yield similar to methanol would be expected (see data on Table 1). The difference found in the hydrogen efficiencies between methanol and ethanol is due to the known lower efficiency of ethanol as hole scavenger compared to a smaller alcohol molecule such as methanol [47]. In a very recent work [54], photocatalytic applications of 1D monocrystalline TiO_2 nanostructures impregnated with Pt by sputtering were reported. The authors ascribe the high activity of the photocatalysts to the small size of the Pt NPs and the geometry of the obtained TiO_2 films.

Hydrogen production rates were much higher using Pt/TiO_2 NTs than using pure TiO_2 NTs and a clear dependence on the excitation wavelength was observed (see third column in Table 2). Table 2 shows that the Φ_{app} for Pt loaded TiO_2 NTs increased 12% at 254 nm and 16% at 313 nm compared with NTs without Pt NPs. On the contrary Φ_{app} measured at 365 nm was only 1% times. The optical properties of our TiO_2 TNs and Au NPs/TiO_2 NTs were already characterized in a previous publications by UV–vis spectroscopy [39]. In spite in the present work a detailed UV–vis investigation was not carried out for Pt NPs deposited on the TiO_2 NTs, recent publications have reported UV–vis absorbance spectra of Pt NPs loaded on TiO_2 nanostructures [54,59]. Taken into account the increase in the absorbance of TiO_2 and Pt/TiO_2 systems with the decrease in the excitation wavelength, a ratio of 1,43 and 1,37 can be calculated for the ratios $Abs_{(313\ nm)}/Abs_{(365\ nm)}$ and $Abs_{(254\ nm)}/Abs_{(365\ nm)}$ respectively for 1 wt% nominal rate ratio of Pt to Ti [59]. Similar result was obtained by An et al. for the ratio $Abs_{(313\ nm)}/Abs_{(365\ nm)} \sim 1.5$ [54]. Based on the above information, changes in light absorption cannot explain the obtained results because the hydrogen apparent quantum yields increased 16% (313 nm) and 12% (254 nm) compared to 365 nm excitation. The high Φ_{app} obtained at shorter wavelength can be understood taking into account that the mobility of electron–hole pairs affects the photocatalytic activity as well as the conduction band level because it affects the probability of electrons and holes reaching reaction sites on the surface. Those effects have already been observed in tantalate photocatalysts with a higher conduction band level of Ta5d than the reduction potential of water [60]. A key issue in charge separation relates to the energy of the charge carriers formed after photon absorption. "Deep" holes and "hot" electrons are more like to separate than charge carriers generated with near-band gap energy light [1]. Grela et al. [61,62] were the first to examine the photodegradation quantum yields as a function of excitation energy. In one of their works they examined the dependence of the quantum yield for 3-nitrophenol photooxidation [62] on the excess of photon energy (E_{PE}) defined as the photon energy in excess of the TiO_2 band gap energy. The photodegradation quantum yield started to increase significantly over 0.4–0.5 E_{PE} reaching a constant value at ~2.5% over ~0.8 E_{PE}. Our results using Pt loaded TiO_2 NTs catalyst can be interpreted in similar fashion. At 365 nm the E_{PE} is about 0.2 and the Φ_{app} is 1%. On the contrary, at 313 and 254 nm the E_{PE} are 0.76 and 1.68 reaching probably some steady state condition. At higher excitation energies the life time of electrons and holes will probably increase, reaching the surface more easily and therefore increasing the hydrogen quantum yield.

Finally, Table 2 shows a difference in the Φ_{app} between 254 and 313 nm of excitation energy. Previous studies on photocatalyzed degradation of phenol and 4-chlorophenol have shown that in both cases, the reactions displayed a well-defined spectral dependence with some fine structure in the quantum yields measured [63]. The spectral dependence was explained because the photogenerated carriers were formed in different states and they have different recombination constants (i.e., different recombination crosssections), and consequently different lifetimes, mobilities, and rate constants for the surface reactions. Our results may show similar

Table 2 – Apparent quantum yield of hydrogen generation on TiO_2 NTs and Pt/TiO_2 NTs at selected wavelengths in a mixtures of methanol/water or ethanol/water 1/8 (v/v).

λ (nm)	$\phi_{H_2} \times 100$			
	Methanol/water		Ethanol/water	
	TiO_2 NTs	Pt loaded TiO_2 NTs	Pt loaded TiO_2 NTs/TiO_2 NTs	Pt loaded TiO_2 NTs
254	≤0.1	12 ± 2	120	8 ± 1
313	>0.02	16 ± 2	800	–
365	~0.02	1 ± 0.1	50	–

spectral dependence, but further studies would be needed to confirm that hypothesis for the hydrogen photogeneration on Pt loaded TiO_2 NTs.

4. Conclusions

In summary, the results presented here are very promising because hydrogen can be produced at ambient conditions via an efficient, technologically simple, ecologically benign and potentially very low-cost process. Indeed, the system uses simple Pt-loaded TiO_2 NTs photocatalyst and abundant and renewable sources: alcohols and water. Pt loading on TiO_2 NTs was highly efficiently in hydrogen generation. The apparent quantum yield in hydrogen formation measured at 313 nm was about 16%. The clear dependence of the apparent hydrogen quantum yield on the excitation wavelength showed that this experimental parameter should be taking into account for the optimization of an efficient hydrogen production system. The obtained results showed that the approach developed in the present work has the potential to produce hydrogen via photocatalysis in enough amounts from a point of view of a potential application. Simultaneously, it was clearly shown the known intrinsic difficulty of TiO_2 semiconductor that it is to produce hydrogen efficiently by solar light harvesting. Even if Pt is used as co-catalyts, the highest apparent hydrogen quantum yields were obtained at wavelengths where the of solar radiation flux in the UV region reaching the Earth surface is minimum or zero. Therefore, new catalysts materials are needed to allow harvesting of solar light. Moreover, the Pt DC-MS method reported herein represents a simple and efficient method for the metalation of semi-conductors of all types, shapes and sizes that can be easily employed in the expected future generation of visible light photocatalysts for the WS reaction.

Acknowledgment

This work was partially sponsored by CNPq, CAPES and ANEEL-CEEE GT (no. 9945481). Thanks to CME (UFRGS), LNLS – National Synchrotron Light Laboratory, Brazil (TGM beam line), INMETRO and Dr. Heberton Wender for his collaboration on GAXRD measurements in XRD-2 beam line.

Appendix A. Supplementary data

Supplementary data related to this article can be found at http://dx.doi.org/10.1016/j.ijhydene.2013.09.018.

REFERENCES

[1] Henderson MA. A surface science perspective on TiO_2 photocatalysis. Surf Sci Rep 2011;66:185–297.
[2] Fujishima A, Zhang X, Tryk DA. TiO_2 photocatalysis and related surface phenomena. Surf Sci Rep 2008;63:515–82.
[3] Fujishima A, Honda K. Electrochemical photolysis of water at a semiconductor electrode. Nature 1972;238:37–8.
[4] Bard AJ, Fox MA. Artificial photosynthesis: solar splitting of water to hydrogen and oxygen. Acc Chem Res 1995;28:141–5.
[5] Ni M, Leung MKH, Leung DYC, Sumathy K. A review and recent developments in photocatalytic water-splitting using TiO_2 for hydrogen production. Renew Sust Energ Rev 2007;11:401–25.
[6] Nishijima K, Kamai T, Murakami N, Tsubota T, Ohno T. Photocatalytic hydrogen or oxygen evolution from water over S- or N-doped TiO_2 under visible light. Int J Photoenergy 2008;2008:1–7.
[7] Zou JJ, Chen C, Liu CJ, Zhang YP, Han Y, Cui L. Pt nanoparticles on TiO_2 with novel metal-semiconductor interface as highly efficient photocatalyst. Mater Lett 2005;59:3437–40.
[8] Patsoura A, Kondarides DI, Verykios XE. Photocatalytic degradation of organic pollutants with simultaneous production of hydrogen. Catal Today 2007;124:94–102.
[9] Oppenlander T, Gliese S. Mineralization of organic micropollutants (homologous alcohols and phenols) in water by vacuum-UV-oxidation (H_2O-VUV) with an incoherent xenon-excimer lamp at 172 nm. Chemosphere 2000;40:15–21.
[10] Daskalaki VM, Kondarides DI. Efficient production of hydrogen by photo-induced reforming of glycerol at ambient conditions. Catal Today 2009;144:75–80.
[11] Bamwenda GR, Tsubota S, Kobayashi T, Haruta M. Photoinduced hydrogen-production from an aqueous-solution of ethylene-glycol over ultrafine gold supported on TiO_2. J Photoch Photobio A 1994;77:59–67.
[12] Stjohn MR, Furgala AJ, Sammells AF. Hydrogen generation by photocatalytic oxidation of glucose by platinized N-TiO_2 powder. J Phys Chem 1983;87:801–5.
[13] Wang YD, Zhang AM, Xu QH, Chen RZ. Characterization of titanium-modified USY zeolites and their catalytic performance on n-heptane cracking. Appl Catal A-Gen 2001;214:167–77.
[14] Li YX, Me YZ, Peng SQ, Lu GX, Li SB. Photocatalytic hydrogen generation in the presence of chloroacetic acids over Pt/TiO_2. Chemosphere 2006;63:1312–8.
[15] Kondarides DI, Daskalaki VM, Patsoura A, Verykios XE. Hydrogen production by photo-induced reforming of biomass components and derivatives at ambient conditions. Catal Lett 2008;122:26–32.
[16] Huang B-S, Wey M-Y. Properties and H_2 production ability of Pt photodeposited on the anatase phase transition of nitrogen-doped titanium dioxide. Int J Hydrogen Energy 2011;36:9479–86.
[17] de Tacconi NR, Timmaji HK, Chanmanee W, Huda MN, Sarker P, Janaky C, et al. Photocatalytic generation of syngas using combustion-synthesized silver bismuth tungstate. Chemphyschem 2012;13:2945–55.
[18] Rajeshwar K. Solar energy conversion and environmental rennediation using inorganic semiconductor-liquid interfaces: the road traveled and the way forward. J Phys Chem Lett 2011;2:1301–9.
[19] Gaertner F, Losse S, Boddien A, Pohl M-M, Denurra S, Junge H, et al. Hydrogen evolution from water/alcohol mixtures: effective in situ generation of an active Au/TiO_2 catalyst. Chemsuschem 2011;5:530–3.
[20] Gomathisankar P, Yamamoto D, Katsumata H, Suzuki T, Kaneco S. Photocatalytic hydrogen production with aid of simultaneous metal deposition using titanium dioxide from aqueous glucose solution. Int J Hydrogen Energy 2013;38:5517–24.
[21] Seh ZW, Liu S, Low M, Zhang S-Y, Liu Z, Mlayah A, et al. Janus Au–TiO_2 photocatalysts with strong localization of plasmonic near-fields for efficient visible-light hydrogen generation. Adv Mater 2012;24:2310–4.

[22] Lin HY, Chang YS. Photocatalytic water splitting for hydrogen production on Au/KTiNbO$_5$. Int J Hydrogen Energy 2010;35:8463–71.
[23] Lai Y, Gong J, Lin C. Self-organized TiO$_2$ nanotube arrays with uniform platinum nanoparticles for highly efficient water splitting. Int J Hydrogen Energy 2012;37:6438–46.
[24] D'Elia D, Beauger C, Hochepied J-Fo, Rigacci A, Berger M-Hln, Keller N, et al. Impact of three different TiO$_2$ morphologies on hydrogen evolution by methanol assisted water splitting: nanoparticles, nanotubes and aerogels. Int J Hydrogen Energy 2011;36:14360–73.
[25] Rosseler O, Shankar MV, Du MKL, Schmidlin L, Keller N, Keller V. Solar light photocatalytic hydrogen production from water over Pt and Au/TiO$_2$(anatase/rutile) photocatalysts: influence of noble metal and porogen promotion. J Catal 2010;269:179–90.
[26] Kandiel TA, Dillert R, Robben L, Bahnemann DW. Photonic efficiency and mechanism of photocatalytic molecular hydrogen production over platinized titanium dioxide from aqueous methanol solutions. Catal Today 2011;161:196–201.
[27] Ismail AA, Bahnemann DW, Rathousky J, Yarovyi V, Wark M. Multilayered ordered mesoporous platinum/titania composite films: does the photocatalytic activity benefit from the film thickness? J Mater Chem 2011;21:7802–10.
[28] Fateh R, Ismail AA, Dillert R, Bahnemann DW. Highly active crystalline mesoporous TiO$_2$ films coated onto polycarbonate substrates for self-cleaning applications. J Phys Chem C 2011;115:10405–11.
[29] Merka O, Bahnemann DW, Wark M. Improved photocatalytic hydrogen production by structure optimized nonstoichiometric $Y_2Ti_2O_7$. ChemCatChem 2012;4:1819–27.
[30] Nam W, Han GY. Preparation and characterization of anodized Pt–TiO$_2$ nanotube arrays for water splitting. J Chem Eng Jpn 2007;40:266–9.
[31] Lee WJ, Alhosan M, Yohe SL, Macy NL, Smyrlz WH. Synthesis of Pt/TiO$_2$ nanotube catalysts for cathodic oxygen reduction. J Electrochem Soc 2008;155:B915–20.
[32] Bamwenda GR, Tsubota S, Nakamura T, Haruta M. Photoassisted hydrogen-production from a water-ethanol solution - a comparison of activities of Au-Tio$_2$ and Pt-Tio$_2$. J Photoch Photobio A 1995;89:177–89.
[33] Herrmann JM, Disdier J, Pichat P. Photoassisted platinum deposition on Tio$_2$ powder using various platinum complexes. J Phys Chem 1986;90:6028–34.
[34] Huang BS, Chang FY, Wey MY. Photocatalytic properties of redox-treated Pt/TiO$_2$ photocatalysts for H$_2$ production from an aqueous methanol solution. Int J Hydrogen Energy 2010;35:7699–705.
[35] Naseri N, Sangpour P, Moshfegh AZ. Visible light active Au:TiO$_2$ nanocomposite photoanodes for water splitting: sol–gel vs. sputtering. Electrochim Acta 2011;56:1150–8.
[36] Esposito DV, Hunt ST, Stottlemyer AL, Dobson KD, McCandless BE, Birkmire RW, et al. Low-cost hydrogen-evolution catalysts based on monolayer platinum on tungsten monocarbide substrates. Angew Chem Int Edit 2010;49:9859–62.
[37] Goncalves RV, Migowski P, Wender H, Eberhardt D, Weibel DE, Sonaglio FvC, et al. Ta_2O_5 nanotubes obtained by anodization: effect of thermal treatment on the photocatalytic activity for hydrogen production. J Phys Chem C 2012;116:14022–30.
[38] Wender H, Feil AF, Diaz LB, Ribeiro CS, Machado GJ, Migowski P, et al. Self-organised TiO$_2$ nanotube arrays: synthesis by anodization in an ionic liquid and assessment of photocatalytic properties. Appl Mater Interfaces 2011;3:1359–65.
[39] Feil AF, Migowski P, Pierozan MD, Corsetti RR, Scheffer FR, Rodrigues M, et al. Growth of TiO$_2$ nanotube arrays with simultaneous Gold impregnation: photocatalysts for hydrogen production. J Braz Chem Soc 2010;21:1359–65.
[40] Feil AF, Weibel DE, Corsetti RR, Pierozan MD, Michels AF, Horowitz F, et al. Micro and nano-texturization of intermetallic oxide alloys by a single anodization step: preparation of artificial self-cleaning surfaces. Appl Mater Interfaces 2011;3:3981–7.
[41] Rodriguezcarvajal J. Recent advances in magnetic-structure determination by neutron powder diffraction. Physica B 1993;192:55–69.
[42] McCusker LB, Von Dreele RB, Cox DE, Louer D, Scardi P. Rietveld refinement guidelines. J Appl Crystallogr 1999;32:36–50.
[43] Dollase WA. Correction of intensities for preferred orientation in powder diffractometry - application of the March model. J Appl Crystallogr 1986;19:267–72.
[44] Calvert JG, Pitts JN. Photochemistry. New York: John Wiley; 1966.
[45] Sen F, Gokagac G. Different sized platinum nanoparticles supported on carbon: an XPS study on these methanol oxidation catalysts. J Phys Chem C 2007;111:5715–20.
[46] Highfield JG, Chen MH, Nguyen PT, Chen Z. Mechanistic investigations of photo-driven processes over TiO$_2$ by in-situ DRIFTS-MS: part 1. Platinization and methanol reforming. Energy Environ Sci 2009;2:991–1002.
[47] Tamaki Y, Furube A, Murai M, Hara K, Katoh R, Tachiya M. Direct observation of reactive trapped holes in TiO$_2$ undergoing photocatalytic oxidation of adsorbed alcohols: evaluation of the reaction rates and yields. J Am Chem Soc 2006;128:416–7.
[48] Mota CJA, da Silva CXA, Gonçalves VLC. Gliceroquímica: novos produtos e processos a partir da glicerina de produção de biodiesel. Quim Nova 2009;32:639–48.
[49] Bahruji H, Bowker M, Davies PR, Al-Mazroai LS, Dickinson A, Greaves J, et al. Sustainable H$_2$ gas production by photocatalysis. J Photoch Photobio A 2010;216:115–8.
[50] Chatterjee D, Dasgupta S. Visible light induced photocatalytic degradation of organic pollutants. J Photoch Photobio C 2005;6:186–205.
[51] Ortiz-Gomez A, Serrano-Rosales B, de Lasa H. Enhanced mineralization of phenol and other hydroxylated compounds in a photocatalytic process assisted with ferric ions. Chem Eng Sci 2008;63:520–57.
[52] Guo CS, Ge M, Liu L, Gao GD, Feng YC, Wang YQ. Directed synthesis of mesoporous TiO$_2$ microspheres: catalysts and their photocatalysis for bisphenol a degradation. Environ Sci Technol 2010;44:419–25.
[53] Mahapure SA, Rane VH, Ambekar JD, Nikam LK, Marimuthu R, Kulkarni MV, et al. Novel solar light driven photocatalyst, zinc indium vanadate for photodegradation of aqueous phenol. Mater Res Bull 2011;46:635–8.
[54] An W-J, Wang W-N, Ramalingam B, Mukherjee S, Daubayev B, Gangopadhyay S, et al. Enhanced water photolysis with Pt metal nanoparticles on single crystal TiO$_2$ surfaces. Langmuir 2012;28:7528–34.
[55] Okabe H. Photochemistry of small molecules. New York: John Wiley & Sons; 1978.
[56] Turro JN. Modern molecular photochemistry. California: The Benjamin/Cummings Publilshing Company, Inc.; 1978.
[57] Serpone N. Relative photonic efficiencies and quantum yields in heterogeneous photocatalysis. J Photoch Photobio A 1997;104:1–12.
[58] Navarro Yerga RM, Alvarez Galvan MC, del Valle F, Villoria de la Mano JA, Fierro JLG. Water splitting on semiconductor catalysts under visible-light irradiation. Chemsuschem 2009;2:471–85.

[59] Yu JG, Qi LF, Jaroniec M. Hydrogen production by photocatalytic water splitting over Pt/TiO_2 nanosheets with exposed (001). Facets J Phys Chem C 2010;114:13118–25.
[60] Kudo A, Miseki Y. Heterogeneous photocatalyst materials for water splitting. Chem Soc Rev 2009;38:253–78.
[61] Grela MA, Colussi AJ. Photon energy and photon intermittence effects on the quantum efficiency of photoinduced oxidations in crystalline and metastable TiO_2 colloidal nanoparticles. J Phys Chem B 1999;103:2614–9.
[62] Grela MA, Brusa MA, Colussi AJ. Efficiency of hot carrier trapping by outer-sphere redox probes at quantum dot interfaces. J Phys Chem B 1999;103:6400–2.
[63] Emeline A, Salinaro A, Serpone N. Spectral dependence and wavelength selectivity in heterogeneous photocatalysis. I. Experimental Evidence from the photocatalyzed transformation of phenols. J Phys Chem B 2000;104:11202–10.